Dynamic responses of a two-dimensional flapping foil motion

Xi-Yun Lu[a] and Qin Liao
Department of Modern Mechanics, University of Science and Technology of China, Hefei, Anhui 230026, China

(Received 5 June 2006; accepted 25 August 2006; published online 27 September 2006)

The investigation of a flapping foil, which is used as a basic mode of the flapping-based locomotion in insects, birds, and fish, is performed by solving the Navier-Stokes equations numerically. In this Brief Communication we provide insight into the understanding of dynamics of a flapping foil. A critical flapping Reynolds number based on the flapping frequency and amplitude, above which a forward flapping movement occurs, is predicted. The dynamics of the flapping foil are analyzed in two dynamic responses, i.e., an oscillatory movement and a steady movement, which depend on the density ratio between the foil and the surrounded fluid. The steady movement response is related to the forward flapping motion. The Strouhal number that governs a vortex shedding for the forward flapping foil is calculated and lies in the range where flying and swimming animals will be likely to tune for high propulsive efficiency. © *2006 American Institute of Physics*.
[DOI: 10.1063/1.2357733]

The mechanism of natural locomotion is a central question for flying and swimming animals. Theoretical treatments were proposed typically for the Stokesian (or low Reynolds number approximation) and the Eulerian (or high Reynolds number approximation) regimes.[1–4] More recently, the swimming of animalcules in a viscous fluid at low Reynolds number is analyzed by the nonlinear equations of Stokesian dynamics.[5] However, numerous animals locomote in the range of the intermediate Reynolds number. The mechanisms of locomotion appropriate to this Reynolds number range do not fall fully within the scope of either Stokesian or Eulerian theory. Therefore, it is highly desired to reveal the relevant mechanisms of locomotion based on some typical models.

A two-dimensional flapping foil, which is usually used as a basic mode of locomotion in flying and swimming animals,[6,7] is considered here. Although we recognize the limitation of this model, we nevertheless feel that the results will be of help in physical understanding of the relevant mechanisms in the flapping-based locomotion of flying and swimming animals. As shown in Fig. 1(a), the vertical position of the flapping foil is given by

$$h(t) = \bar{A}\cos(2\pi f t), \tag{1}$$

where $\bar{A}$ and f are the flapping amplitude and frequency, respectively. Then, a flapping Reynolds number is defined as $\mathrm{Re}_A = \rho_\omega f \bar{A} c/\mu$, where c is the chord of foil, ρ_0 the fluid density, and μ the dynamic viscosity.

Based on this model, some studies have been performed experimentally and numerically. Vandenberghe, Zhang and Childress[8] carried out an experiment to address the threshold value of the flapping Reynolds number above which the transition to forward flapping flight from a pure flapping state occurs. Recently, Alben and Shelley[9] also took a numerical study to reveal the dynamics of the flapping foil and their relation to the foil shape and mass. They only considered one flapping amplitude (i.e., $\bar{A}/c=0.5$) for simplifying the problem, and had somewhat less emphasis on computing the critical flapping Reynolds number. As the critical flapping Reynolds number is exceeded, the flapping foil begins to move spontaneously in the horizontal direction, including a complicated interaction of the foil with the surrounding fluid flow.[8,9] The foil exerts forces on the fluid through its own inertia response and is likewise acted on by the fluid flow pressure and viscous friction. Such fundamental fluid-body interactions are also well shown in the dynamic responses of flexible filaments in a flowing soap film[10] and flag oscillations in fluid flow,[11,12] depending on the filament or flag mass. The goal of this Brief Communication is, over the $(\bar{A}, f)$ parameter space, to examine the critical flapping Reynolds number, the Strouhal number for the forward flapping foil, and the effect of the foil mass on the dynamic responses of the flapping foil.

To simulate flow around an up-and-down flapping foil, we solve the two-dimensional Navier-Stokes equations,

$$\nabla \boldsymbol{u} = 0, \tag{2}$$

$$\frac{\partial \boldsymbol{u}}{\partial t} + \boldsymbol{u}\nabla\boldsymbol{u} = -\nabla p + \frac{\mu}{\rho_0}\nabla^2\boldsymbol{u}, \tag{3}$$

where $\boldsymbol{u}$ is the velocity vector, and p is the pressure. When a foil takes only up-and-down flapping without the horizontal movement, by using c and fc as the characteristic length and velocity to nondimensionalize the equations, two typical dimensionless parameters involved in this problem are the frequency parameter, or frequency Reynolds number, defined as $\beta = \rho_0 f c^2/\mu$, and the flapping amplitude $A = \bar{A}/c$, with a relation to the flapping Reynolds number $\mathrm{Re}_A = \beta A$. The equations are solved by a fractional-step velocity correction method coupled with a finite element spatial discretization.[13]

[a]Author to whom correspondence should be addressed. Electronic mail: xlu@ustc.edu.cn

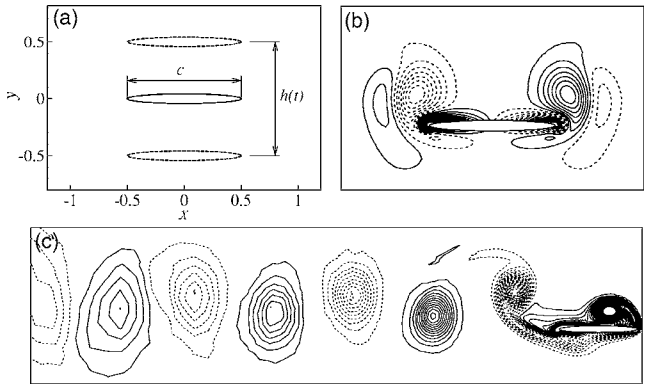

FIG. 1. (a) Sketch of a flapping foil. The foil is an elliptic shape with the thickness-chord ratio 1/12. (b) Vorticity contours in the symmetrical region. Solid lines represent positive values and dashed lines negative values. (c) Vorticity contours in the asymmetric region.

An instantaneous inertial frame technique is used to treat the foil motion.[14] The relevant code was extensively validated and verified to ensure the numerical accuracy and convergence.[15,16]

To identify the boundary between symmetrical and asymmetric flow regime on the $\beta-A$ plane, for each pair of β and A under examination, the horizontal force component F_x is calculated during the flapping cycles. When F_x vanishes always during the cycles, the flow is symmetric with the flow structure being left-right symmetric, as typically shown in Fig. 1(b). When F_x is nonzero, the flow is characterized as asymmetric, the foil will move spontaneously in the horizontal direction. As the foil takes a steady movement along one direction, depending on the foil mass discussed below, vortex shedding occurs with a reverse von Kármán vortex street shown in Fig. 1(c). This behavior is well consistent with the experimental and numerical findings.[6,8,9] After a series of tests with a large number of β and A pairs, the boundary between symmetrical and asymmetric flow regime on the $\beta-A$ plane shown in Fig. 2(a) is determined in the form of a fitting curve, $A=1.9\beta^{-0.57}$. Then, by $\mathrm{Re}_A=\beta A$, the critical flapping Reynolds number can be expressed as approximately

$$\mathrm{Re}_A^c = 3.1A^{-0.75}. \tag{4}$$

Our predicted result, as shown in Fig. 2(b) for the curve of Re_A^c, is consistent with the critical Reynolds number range from observations of swimming and flying animals,[17,18] among others. Further, based on numerical tests, the foil shape with the thickness-chord ratio of less than 15%, in which the relative scales of of swimming and flying animals lie, has a small influence on the boundary. Following our calculations, the critical flapping Reynolds number somewhat becomes smaller with a decrease of the thickness-chord ratio. This behavior is also confirmed by the analysis of linear instability for several thickness-chord ratios.[9]

To analyze the dynamic response of spontaneously moving foil, the flapping frequency and amplitude are chosen in asymmetric regime in Fig. 2. In this case, the horizontal force component F_x, due to the pressure and friction forces

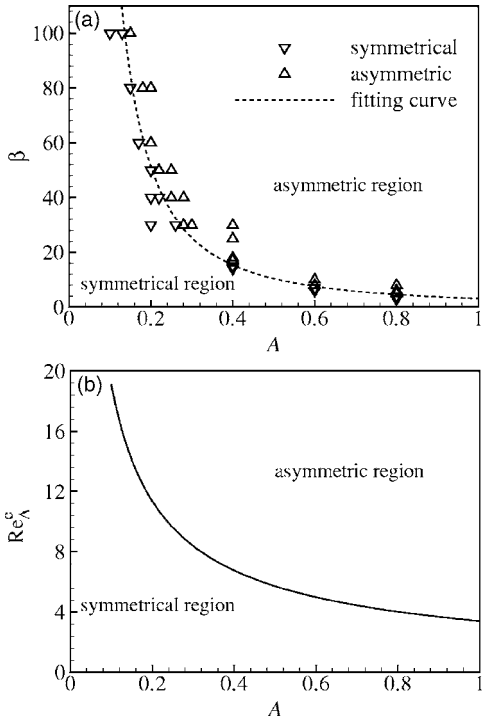

FIG. 2. Boundary between symmetrical and asymmetric flow: (a) $\beta-A$ plane; (b) Re_A^c-A plane. Symbols $\triangle$ and $\triangledown$, corresponding to some typical cases calculated here, represent symmetrical and asymmetric flow, respectively.

exerting on the foil from the surrounding fluid, propels the foil to move horizontally through Newton's second law,

$$m_s\frac{d^2x_s}{dt^2} = F_x, \tag{5}$$

where x_s is the horizontal location of the foil, and m_s is the foil mass per unit spanwise length, or $\rho_s S$, with ρ_s the foil density and S the foil area. To normalize Eq. (5) by $\rho_0 f^2 c^3$, a typical parameter, the density ratio $\sigma=\rho_s/\rho_0$, is introduced.

Here, we deal with the dynamics of the foil with different density ratios. The horizontal locations of the foil at several σ values are shown in Fig. 3. As $\sigma\leqslant 2.2$, the foil undergoes spontaneous oscillations, while as $\sigma\geqslant 2.5$, the foil moves to a stable state and reaches a steady movement after

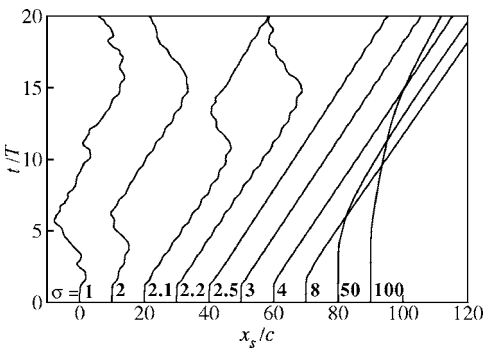

FIG. 3. The horizontal locations x_s/c of the foil at several σ values for $A=0.5$ and $\beta=100$. Here, T is the flapping period. Each location from $\sigma=2$ for the sequence of the σ value shown here is added continuously by an interval 10 to clearly exhibit these curves.

3 to 30 (for $\sigma=100$ in Fig. 3) flapping cycles. Similar dynamic behaviors were also found by Alben and Shelley.[9] Note that the foil can move in either direction for different pairs of β and A, lying in the asymmetric region in Fig. 2; once the direction is chosen, it does not change. It is verified that a threshold value of the density ratio σ_c, e.g., $\sigma_c \sim 2.2-2.5$ for the case in Fig. 3, exists for each pair of β and A. Thus, the horizontal movements of the foil demonstrate the existence of two dynamic responses. One is an oscillatory state when $\sigma<\sigma_c$ and the other a steady movement state when $\sigma>\sigma_c$. After extensive tests with different β and A pairs as well as different σ values, we have also found that σ_c becomes relatively small with increasing β and large with increasing A. The former behavior for σ_c vs β is well consistent with the results,[9] however, the latter for σ_c vs A has not been shown in Ref. 9, since only one flapping amplitude was considered there. The threshold values of the density ratio are $\sigma_c \sim 2-4$ for all cases in the (β,A) parameter space. As a typical case with the thickness-chord ratio 0.1,[9] σ_c is around 3, lying in the range of σ_c predicted in this study. When $\sigma>\sigma_c$, the speed stays constant to within 3% with σ up to 10^2, and the wake of the foil in a steady movement state exhibits a reverse von Kármán vortex street, as shown in Fig. 1(c).

When a foil moves through a fluid, the foil undergoes viscous and inertial forces. The above mechanism immediately suggests that the foil inertia must be increased to overcome fluid viscous force to enter into a steady movement state, otherwise into an oscillatory state. Recently, a similar mechanism was revealed for flexible filaments in a flowing soap film[10] and flag oscillations in fluid flow.[11,12] The above findings also demonstrate that the dynamics of flying and swimming animals involves a complicated interaction of their bodies with the surrounding fluid flow. Usually, real tail or wing of swimming and flying animals has a density ratio $\sigma \sim 10^1-10^3$, so that the flapping mode can naturally stay in the regime of a steady movement state to generate a forward flapping flight.

The tail or wing kinematics of swimming and flying animals are well relevant to the Strouhal number, which is described as $\mathrm{St}=A_w f/U$, where U is the average forward speed and A_w is the width of the wake, taken to be equal to the maximum excursion of the foil's trailing edge, i.e., double amplitude $A_w=2\bar{A}$.[19] The Strouhal number is known to govern a well-defined series of vortex growth and shedding regimes for the flapping foil, or a reverse von Kármán vortex street shown in Fig. 1(c). To characterize the forward speed U, or $U=dx_s/dt$ from Eq. (5) after the foil begins to move steadily, a forward Reynolds number is usually defined as $\mathrm{Re}_U=\rho_o Uc/\mu$. Then, the Strouhal number is also expressed as $\mathrm{St}=2\,\mathrm{Re}_A/\mathrm{Re}_U$.

Computations are carried out for a certain A (or β) with changing β (or A), which lie in the asymmetric region in Fig. 2. The curves of $\mathrm{Re}_A-\mathrm{Re}_U$ are shown in Fig. 4. The relations between Re_A and Re_U are nearly linear for fixed A or β, consistent with the experimental measurements.[8] We identify that St is within the interval 0.2–0.4 approximately, at which flying and swimming animals cruise driven by the wing or tail is likely to tune for high propulsive efficiency because of natural selection.[20] Compared with the predicted St with slightly less than 0.2,[9] which is at the lower end of the range $0.2<\mathrm{St}<0.4$,[20] the present St values shown in Fig. 4 are mostly in the range of 0.25–0.3.

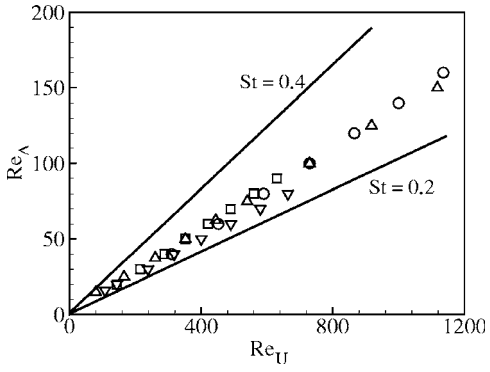

FIG. 4. The forward Reynolds number Re_U versus the flapping Reynolds number Re_A. The Strouhal number is $\mathrm{St}=2\,\mathrm{Re}_A/\mathrm{Re}_U$. Here, ∇ denotes the data for $A=0.2$ with changing β, $\triangle$ for $A=0.5$ with changing β, $\square$ for $\beta=100$ with changing A, and $\bigcirc$ for $\beta=200$ with changing A, respectively.

In summary, based on numerical analysis on a flapping foil over an extensive (β,A) parameter space, the critical flapping Reynolds number is predicted and expressed approximately by (4). The dynamics of the flapping foil are analyzed in two dynamic responses, i.e., an oscillatory movement and a steady movement, which depend on the density ratio σ. The threshold value of the density ratio σ_c is in the range of 2–4 for all cases in the (β,A) parameter space considered here, and becomes relatively small with increasing β and large with increasing A. When $\sigma>\sigma_c$, the flapping mode stays in the regime of the steady movement state to generate a forward flapping flight, and the wake of the foil exhibits a reverse von Kármán vortex street. The Strouhal number, which governs a well-defined series of vortex shedding (or a reverse von Kármán vortex street here) for the flapping foil, is calculated with $\mathrm{St}\sim 0.2-0.4$ approximately, consistent with the regime selected by flying and swimming animals naturally.

This work was supported by the Innovation Project of the Chinese Academy of Sciences (No. KJCX-SW-L04), the National Natural Science Foundation of China (No. 10332040), and the Program for Changjiang Scholars and Innovative Research Team in University. The authors thank Professor X.-Z. Yin and the referee for valuable comments and X. Zha for performing some calculations.

[1] G. I. Taylor, "Analysis of the swimming of microscopic organisms," Proc. R. Soc. London, Ser. A **209**, 447 (1952).
[2] M. J. Lighthill, *Mathematical Biofluiddynamics* (SIAM, Philadelphia, 1975).
[3] T. Y. Wu, *Swimming and Flying in Nature* (Reinhold, New York, 1975).
[4] S. Childress and R. Dudley, "Transition from ciliary to flapping mode in a swimming mollusc: flapping flight as a bifurcation in Re_ω," J. Fluid Mech. **498**, 257 (2004).
[5] B. U. Felderhof, "The swimming of animalcules," Phys. Fluids **18**, 063101 (2006).
[6] G. C. Lewin and H. Haj-Hariri, "Modelling thrust generation of a two-

dimensional heaving airfoil in a viscous flow," J. Fluid Mech. **492**, 339 (2003).
[7]Z. J. Wang, J. M. Birch, and M. H. Dickinson, "Unsteady forces and flows in low Reynolds number hovering flight: two-dimensional computations vs robotic wing experiment," J. Exp. Biol. **207**, 449 (2004).
[8]N. Vandenberghe, J. Zhang, and S. Childress, "Symmetry breaking leads to forward flapping flight," J. Fluid Mech. **506**, 147 (2004).
[9]S. Alben and M. Shelley, "Coherent locomotion as an attracting state for a free flapping body," Proc. Natl. Acad. Sci. U.S.A. **102**, 11163 (2005).
[10]J. Zhang, S. Childress, A. Libchaber, and M. Shelley, "Flexible filaments in a flowing soap film as a model for one-dimensional flags in a two-dimensional wind," Nature **408**, 835 (2000).
[11]M. Shelley, N. Vandenberghe, and J. Zhang, "Heavy flags undergo spontaneous oscillations in flowing water," Phys. Rev. Lett. **94**, 094302 (2005).
[12]M. Argentina and L. Mahadevan, "Fluid-flow-induced flutter of a flag," Proc. Natl. Acad. Sci. U.S.A. **102**, 1829 (2005).
[13]A. Kovacs and M. Kawahara, "A finite element scheme based on the velocity correction method for the solution of the time-dependent incompressible Navier-Stokes equations," Int. J. Numer. Methods Fluids **13**, 403 (1991).
[14]G. W. Yang, X. Y. Lu, and L. X. Zhuang, "Nonlinear analysis of dynamic stability and its application to the prediction and control of wing rock," J. Aircr. **39**, 84 (2002).
[15]Q. Liao, G. J. Dong, and X. Y. Lu, "Vortex formation and force characteristics of a foil in the wake of a circular cylinder," J. Fluids Struct. **19**, 491 (2004).
[16]J. Z. Wu, Z. L. Pan, and X. Y. Lu, "Unsteady fluid-dynamic force solely in terms of control-surface integral," Phys. Fluids **17**, 098102 (2005).
[17]S. Childress, *Mechanics of Swimming and Flying* (Cambridge University Press, Cambridge, 1981).
[18]J. J. Videler, *Fish Swimming* (Chapman & Hall, London, 1993).
[19]M. S. Triantafyllou, G. S. Triantafyllou, and R. Gopalkrishnan, "Wake mechanics for thrust generation in oscillating foils," Phys. Fluids A **3**, 2835 (1991).
[20]G. Taylor, R. Nudds, and A. Thomas, "Flying and swimming animals cruise at a Strouhal number tuned for high power efficiency," Nature **425**, 707 (2003).